Developmental Cell, Vol. 7, 439–453, September, 2004, Copyright ©2004 by Cell Press

Hmx2 and *Hmx3* Homeobox Genes Direct Development of the Murine Inner Ear and Hypothalamus and Can Be Functionally Replaced by *Drosophila Hmx*

Weidong Wang,[1,4] J. Fredrik Grimmer,[2,5] Thomas R. Van De Water,[2,6] and Thomas Lufkin[1,3,*]

[1]Brookdale Center for Developmental and Molecular Biology
Mount Sinai School of Medicine
One Gustave L. Levy Place
New York, New York 10029

[2]Departments of Otolaryngology and Neuroscience
Albert Einstein College of Medicine
1410 Morris Park Avenue
Bronx, New York 10461

[3]Genome Institute of Singapore
Genome #02-01
60 Biopolis Street
Singapore 138672

Summary

The *Hmx* homeobox gene family appears to play a conserved role in CNS development in all animal species examined, and in higher vertebrates has an additional role in sensory organ development. Here, we show that murine *Hmx2* and *Hmx3* have both overlapping and distinct functions in the development of the inner ear's vestibular system, whereas their functions in the hypothalamic/pituitary axis of the CNS appear to be interchangeable. As in analogous knockin studies of *Otx* and *En* function, *Drosophila Hmx* can rescue conserved functions in the murine CNS. However, in contrast to *Otx* and *En*, *Drosophila Hmx* also rescues significant vertebrate-specific functions outside the CNS. Our work suggests that the evolution of the vertebrate inner ear may have involved (1) the redeployment of ancient *Hmx* activities to regulate the cell proliferation of structural components and (2) the acquisition of additional, vertebrate-specific *Hmx* activities to regulate the sensory epithelia.

Introduction

It has been argued that the diversity and complexity of higher members of the animal kingdom were achieved by systematic duplication and diversification of developmental control genes during the course of evolution (Greer et al., 2000; Holland and Garcia-Fernandez, 1996; Meyer and Schartl, 1999). Following gene duplication and evolutionary selection, multiple members of the same gene family partially retained the function(s) of their ancestral gene while at the same time each individual gene acquired unique capabilities which conferred a selective advantage when tested over long periods of time. These two actions, duplication and diversification, are the primary forces which drive the elaboration of novel developmental pathways, which eventually gave rise to the morphological diversity of the vertebrates during evolutionary time.

Murine *Hmx2* and *Hmx3* are coexpressed in the developing inner ear with the sole exception that *Hmx3* is turned on 8 hr earlier than *Hmx2* within the otic epithelium. In the developing CNS, *Hmx2* and *Hmx3* display an identical temporal and spatial pattern of expression in the developing hypothalamus and neural tube (Wang et al., 2001). The loss of *Hmx3* results in severe vestibular defects characterized by a significant loss of sensory cells in the fused utriculosaccular cavity, as well as a complete absence of the horizontal semicircular duct crista (Wang et al., 1998). Mice lacking *Hmx2* exhibit more severe defects in the inner ear than the *Hmx3* null mice, as the gross morphogenesis of the inner ear is affected. Inactivation of *Hmx2* changes the cell fate in the lateral aspect of the otic epithelium and the adjacent mesenchyme as characterized by a reduced cell proliferation rate, as well as an altered expression of inner ear markers such as *Bmp4*, *Dlx5*, and *Pax2* (Wang et al., 2001). Comparing the inner ear defects displayed by either *Hmx2* or *Hmx*3 null mice, it is notable that not all of the regions coexpressing *Hmx2* and *Hmx3*, such as the saccule, posterior ampulla, and endolymphatic duct (diagrammed in Figures 7Ac and 7Ad), are severely affected in either mutant, suggesting that a possible functional overlap may exist between *Hmx2* and *Hmx3*. Moreover, the absence of overt defects in the nervous system in either the *Hmx2* or *Hmx3* single knockout mice may be related to a functional overlap between those two genes in the CNS, which is evolutionarily a more ancient organ than the inner ear. Both genes are widely expressed in the developing neural tube and hypothalamus (Wang et al., 2001, 2000, 1998).

Invertebrates such as sea urchin or *Drosophila* appear to have only a single *Hmx* gene in their genome (Wang et al., 1990, 2000). An ancestral function of the *Hmx* gene family, as indicated by the *DHmx* expression pattern in *Drosophila*, seems to be involved in the development of the nervous system (Wang et al., 2000). Expression of the *Hmx* genes seems to be conserved among vertebrates (Bober et al., 1994; Rinkwitz-Brandt et al., 1995; Stadler et al., 1992; Stadler and Solursh, 1994; Wang et al., 2000; Yoshiura et al., 1998). The conserved pattern of expression within subdomains of the brain primordia in both *Drosophila* and mouse suggests an original function of the *Hmx* genes in patterning, regionalization, and/or cell type specification of the CNS. In contrast, their expression in the peripheral nervous system, sensory organs, and uterus may represent recently evolved functions of the *Hmx* genes. To investigate which biochemical functions of the *Hmx* genes have been conserved during evolution, we engineered mouse lines in which the *DHmx* and *lacZ* genes were inserted into the *Hmx3* and *Hmx2* loci, respectively. These genetically modified mice (designated $Hmx2^{lacZ/lacZ}$;$Hmx3^{Dki/Dki}$), which fail to

*Correspondence: lufkin@gis.a-star.edu.sg

[4]Present address: Department of Physiology and Cellular Biophysics, Columbia University College of Physicians and Surgeons, 630 West 168th Street, New York, New York 10032.

[5]Present address: Department of Otolaryngology, University of Michigan School of Medicine, Ann Arbor, Michigan 48109.

[6]Present address: University of Miami Ear Institute, 1600 N.W. 10th Avenue, RMSB 3160, Miami, Florida 33136.

produce functional Hmx2 and Hmx3 proteins, instead express *DHmx* in place of mouse *Hmx3* and *lacZ* in the place of *Hmx2*. By comparing the phenotypes displayed by $Hmx2^{lacZ/lacZ};Hmx3^{Dki/Dki}$ mice with those of wild-type, $Hmx2^{-/-}$, $Hmx3^{-/-}$, and $Hmx2^{-/-};Hmx3^{-/-}$ mice, we delineated the conserved biological functions of the *Hmx* genes across the phyla. When substituted for *Hmx3*, *Drosophila Hmx* directed normal development of the hypothalamus and largely rescued the *Hmx3* component of the $Hmx2^{lacZ/lacZ};Hmx3^{Dki/Dki}$ inner ears, indicating that despite significant differences in mouse and fly organ morphogenesis and global body plan development, the functional domains of the Hmx proteins have clearly been conserved and *Drosophila* Hmx is able to recruit the necessary accessory proteins and cofactors to bind murine inner-ear regulatory elements and correctly control downstream targets. Furthermore, these results indicate that the evolution of complex vertebrate organ systems such as the inner ear can result from the cooption of primitive developmental genetic programs into additional embryonic regions, rather than solely through the acquisition or modification of protein functional domains.

Results

Complete Loss of Balance, Postnatal Dwarfism, and Subsequent Lethality in *Hmx2;Hmx3* Null Neonates

Homologous recombination of the targeting construct into the *Hmx2;Hmx3* locus resulted in the deletion of an 11 kb genomic fragment spanning the *Hmx2* and *Hmx3* homeoboxes. Analysis of genomic DNA sequences in the *Hmx2;Hmx3* intervening region revealed no other existing or predicted (Genescan) exonic or gene sequences other than those of *Hmx2* and *Hmx3*. From this mutant allele, the only potential protein product that could be translated is a truncated Hmx3 protein lacking the C-terminal portion of its homeodomain that is essential for DNA binding. This mutation therefore simultaneously created a null allele for both *Hmx2* and *Hmx3*. Germline transmission was achieved with two correctly targeted clones, 391 and 471, resulting in mouse lines with identical phenotypes in all aspects examined regardless of their genetic backgrounds. The $Hmx2^{+/-};Hmx3^{+/-}$ mice showed no obvious physiological or behavioral abnormalities and were fertile. In contrast, the $Hmx2^{-/-};Hmx3^{-/-}$ mice displayed a postnatal lethal phenotype with complete penetrance. Among more than 700 embryos collected from matings between heterozygotes from E8.5 to E18.5, an expected number of wild-type, heterozygotes, and homozygotes (based upon Mendelian inheritance) were present, indicating that $Hmx2^{-/-};Hmx3^{-/-}$ embryos are capable of developing to term. At birth, the $Hmx2^{-/-};Hmx3^{-/-}$ neonates were indistinguishable from their wild-type or heterozygous littermates in size and appearance. From postpartum day 3 (P3) onward, a severe delay in development was observed in the $Hmx2^{-/-};Hmx3^{-/-}$ pups even though ample amounts of milk were found in their stomachs. $Hmx2^{-/-};Hmx3^{-/-}$ mice displayed a complete loss of balance and were unable to right themselves, suggestive of severe vestibular defects, whereas their normal siblings were able to do so at this stage (left panel in Figure 1C). In addition, the $Hmx2^{-/-};Hmx3^{-/-}$ pups exhibited frequent muscle spasms. The majority of $Hmx2^{-/-};Hmx3^{-/-}$ pups died around the 5th day after birth. Less than 10% of the $Hmx2^{-/-};Hmx3^{-/-}$ pups survived until day 9. At the time of death, the $Hmx2^{-/-};Hmx3^{-/-}$ bodies were approximately one-half the length and less than one-third in weight of their normal littermates (right panel in Figure 1C).

Progressive Degeneration of the Entire Vestibular System in the *Hmx2;Hmx3* Mutant Embryos

The semicircular canals of wild-type mice were readily identified using the paint-filling technique and in histological sections. In the $Hmx2^{-/-};Hmx3^{-/-}$ mice, the lateral, superior, and posterior semicircular canals were absent as early as E14.5 (Figures 1Da and 1Db). Histological analysis of the cochlea of the $Hmx2^{-/-};Hmx3^{-/-}$ mice revealed an intact scala vestibule, scala tympani, and scala media with organ of Corti. Analysis of paint-filled specimens also revealed an appropriate degree of cochlear turning for the corresponding embryonic age (Figures 1Da–1Dd). Detailed histological analysis revealed that, in the wild-type mice, the endolymphatic volume of the utricle and saccule grew exponentially between E14.5 and birth (Figure 2B). Even as early as E14.5, the saccule, utricle, and semicircular canals were easily identified in the paint-filled labyrinths (Figure 1Da). The saccule and utricle of the $Hmx2^{-/-};Hmx3^{-/-}$ mice measured less than 5% and 1%, respectively, of the expected volume at E14.5 (saccule, $p = 2.4 \times 10^{-6}$) and E15.5 (utricle, $p = 1.2 \times 10^{-7}$) (Figure 2B). The initial development of the endolymphatic duct and sac appeared to be normal prior to E12.0. However, from E14.5, this structure failed to proliferate, and by E16.5 the overall structure of the vestibular membranous labyrinth was barely identifiable (Figures 1Da–1Dd). By E18.5, the utricle and saccule of the $Hmx2^{-/-};Hmx3^{-/-}$ mice were absent, leaving the cochlear duct in direct communication with the remnant structure of the endolymphatic duct (Figures 1De and 1Df).

In the $Hmx2^{-/-};Hmx3^{-/-}$ mice, the macular area was already greatly diminished at E14.5 to about 20% of the area in the wild-type mice ($p = 1.2 \times 10^{-7}$) and decreased in size until its complete loss by E18.5 (Figure 2A). Histological analysis of the utricular and saccular maculae at E15.5 and E16.5 reveals a diminished population of hair cells by approximately 10^2-fold in the $Hmx2^{-/-};Hmx3^{-/-}$ mice as compared to the wild-type mice (Figure 2C). The density of apoptotic bodies in the maculae of the $Hmx2^{-/-};Hmx3^{-/-}$ was greater by at least 2-fold at E15.5 ($p = 0.01$) and E16.5 ($p = 0.064$) as compared to the wild-type mice (Figure 2E). The density of mitotic figures in the macular sensory epithelium of the $Hmx2^{-/-};Hmx3^{-/-}$ mice was also increased by about 3-fold at E15.5 ($p = 0.02$) and E16.5 ($p = 0.02$) as compared to the wild-type mice (Figure 2D). Since the dramatic reduction in the total number of hair cells in the macular epithelium in the $Hmx2^{-/-};Hmx3^{-/-}$ inner ear, higher mitotic figures suggested that the majority of the remaining cells in the macular epithelium were actively proliferating "progenitor-like" cells that eventually died out via programmed cell death (apoptosis) by postnatal

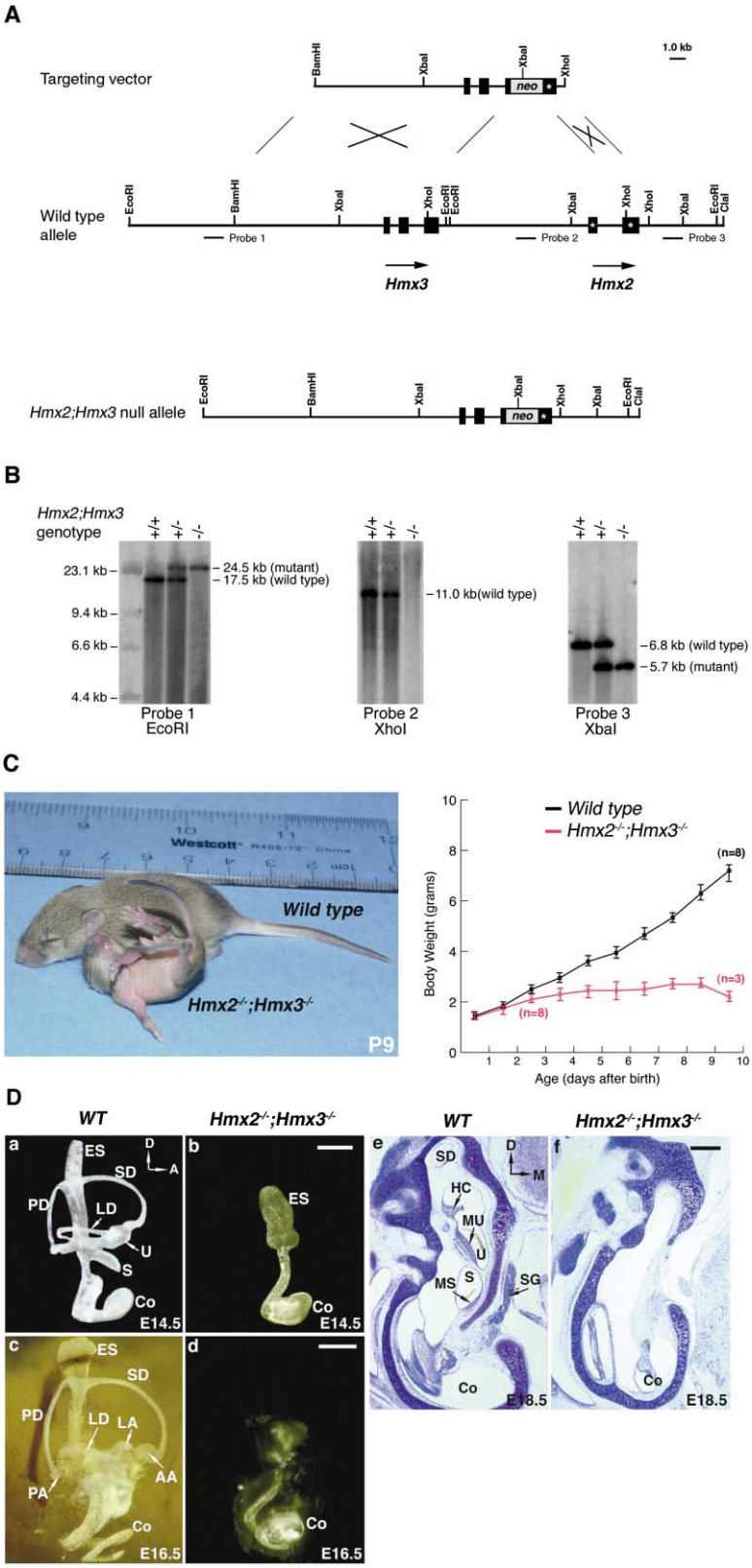

Figure 1. Gene Targeting and Analysis of the *Hmx2* and *Hmx3* Loci

(A) Targeting construct for *Hmx2;Hmx3* double knockout, wild-type locus, and disrupted allele. The arrows show the transcriptional orientation of the *Hmx2* and *Hmx3* genes. The solid rectangle boxes show the position and size of each exon for both genes. Rectangle boxes with stars inside are the exons of *Hmx2* gene.

(B) Southern blot analysis of tailtip DNAs from offspring carrying wild-type, heterozygous, and null alleles for both genes.

(C) $Hmx2^{-/-};Hmx3^{-/-}$ pups show a complete loss of balance and severe growth retardation in their postnatal development. The right panel is the comparison between growth rate curves of wild-type and $Hmx2^{-/-};Hmx3^{-/-}$ pups. In total, eight newborns from each genotype (wild-type or $Hmx2^{-/-};Hmx3^{-/-}$) were used for measuring their bodyweight.

(D) Histological analyses of the inner ear defects displayed by the $Hmx2^{-/-};Hmx3^{-/-}$ embryos. The genotype of each specimen is shown on the top of each column. The embryonic stages are indicated at the lower right corner of each panel. (a to d) Lateral views of paint-filled inner ears from wild-type (a and c), and $Hmx2^{-/-};Hmx3^{-/-}$ (b and d) embryos at E14.5 and E16.5. (e and f) Toluidine blue-stained paraffin sections of E18.5 temporal bones from wild-type and $Hmx2^{-/-};Hmx3^{-/-}$ inner ears. Scale bars in (b) corresponds to 50 μm, in (d) and (f) to 300 μm. Abbreviations: A, anterior; AA, anterior ampulla; Co, cochlea; D, dorsal; ES, endolymphatic sac; HC, horizontal crista; LA, lateral ampulla; LD, lateral semicircular duct; M, medial; MS, macula sacculus; MU, macula utriculus; PA, posterior ampulla; PD, posterior semicircular duct; S, saccule; SD, superior semicircular duct; U, utricle; VG, vestibular ganglion.

day 1 (Figure 2C). It also suggests that the early induction and proliferation of progenitor cells in the maculae might not be affected by the loss of Hmx2 and Hmx3 proteins.

To explore the regulatory hierarchy involving *Hmx2* and *Hmx3*, in situ hybridization was performed on paraffin sections crossing the dorsal part of the otic vesicle

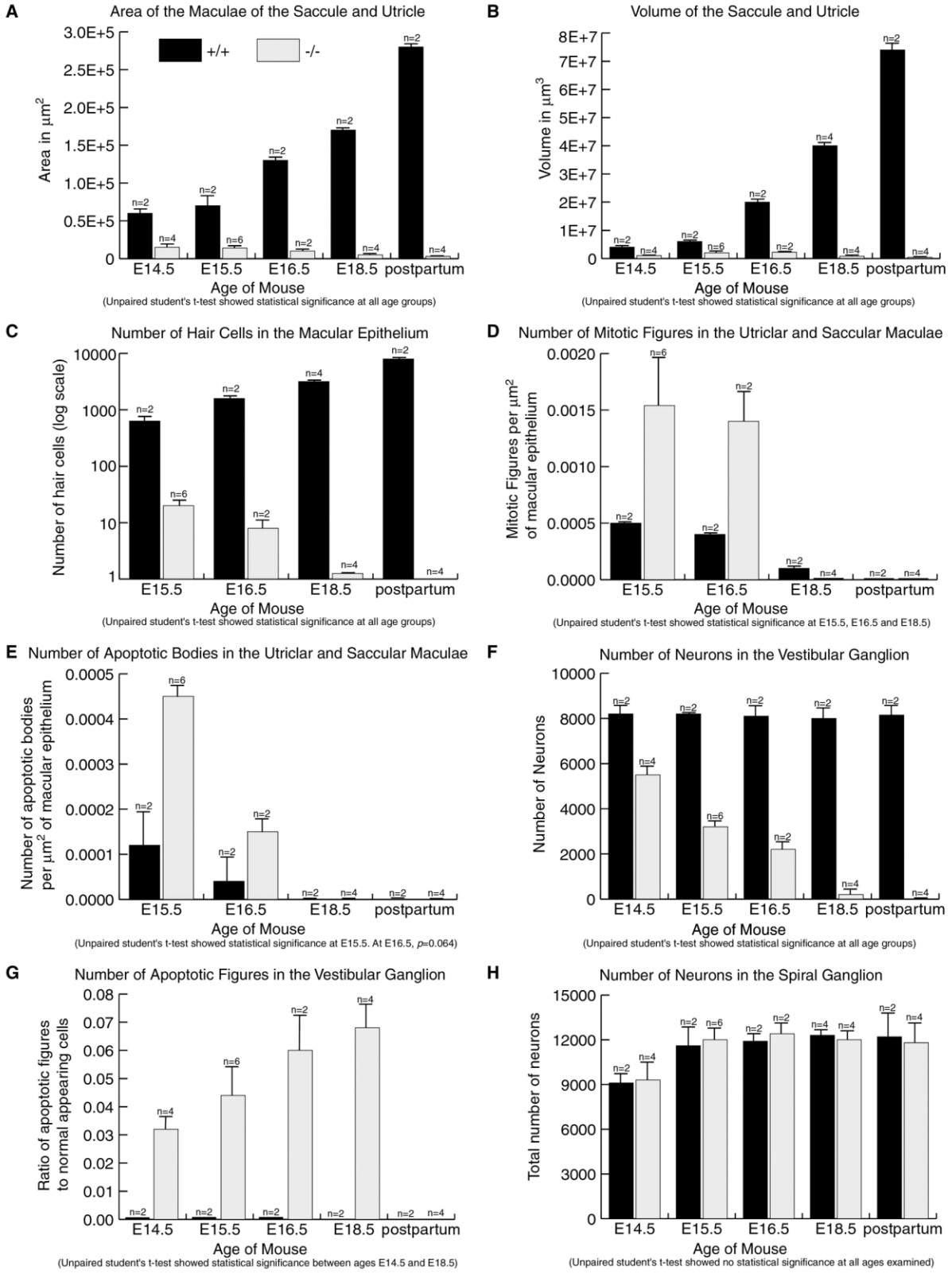

Figure 2. Quantitative Analyses of the Progressive Degeneration of the *Hmx2*$^{-/-}$;*Hmx3*$^{-/-}$ Vestibule and the Associated Ganglion

The black solid boxes represent the wild-type inner ears. Gray, *Hmx2*$^{-/-}$;*Hmx3*$^{-/-}$ inner ears. Statistical analysis was performed using an unpaired Student's t test. Error bars indicate standard deviations. The numbers on the top of each error bar indicate the total number of specimens examined for each assay.

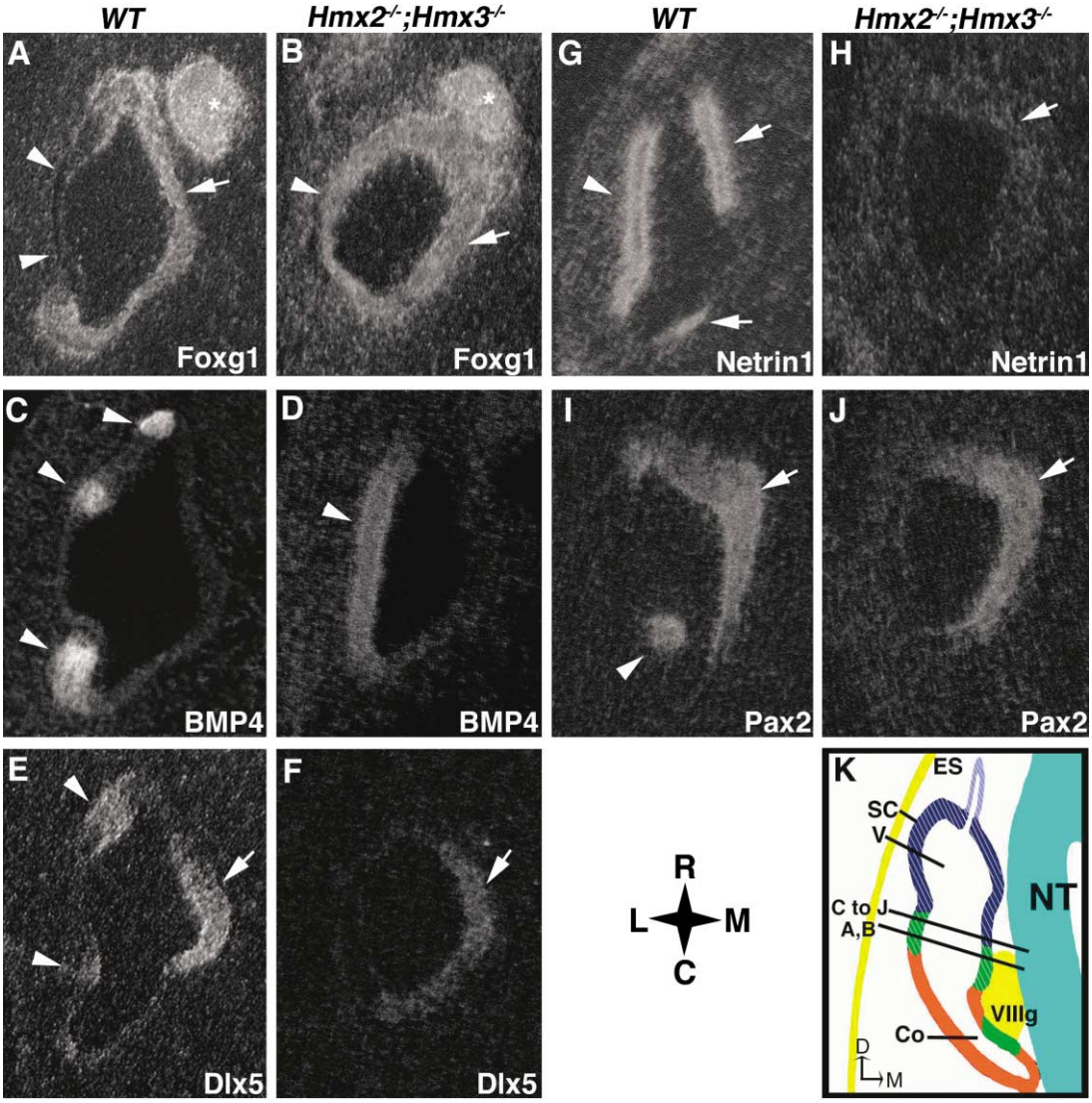

Figure 3. Altered Expression Patterns of Developmental Control Genes in the Otocysts of Wild-Type and *Hmx2*$^{-/-}$;*Hmx3*$^{-/-}$ Embryos at E11.5

The *Hmx2;Hmx3* genotype is indicated on the top of each column. The molecular markers examined are listed on the lower right corner of each panel. (K) shows the corresponding positions of each section. Scale bar in (J) refers to (A) to (J) and corresponds to 50 μm. Abbreviations: C, caudal; L, lateral; M, medial; R, rostral; SC, semicircular canals; V, vestibule; NT, neural tube; VIIIg, facial-acoustic ganglion.

obtained from E11.5 embryos. Like the expression profile in the *Hmx2* mutant inner ear, the wild-type pattern of BMP4 expression in the three prospective clusters of sensory epithelial cells (which would develop into cristae and maculae) was replaced by its uniform presence in the dorsolateral face in the mutant otic vesicle (Figures 3C and 3D). Similarly, disappearance of the *Pax2*-positive domain in the lateral aspect was also observed in the double mutant otic vesicle (arrowhead in Figure 3I), whereas *Pax2* expression in the medial face was correctly maintained (arrows in Figures 3I and 3J). The homeobox gene *Dlx5* is transcriptionally active in three regions in the dorsal otic vesicle, including the developing endolymphatic duct, nonsensory epithelium located between the presumptive anterior and lateral cristae as well as in the region immediately anterior to the putative posterior cristae as marked by *BMP4* (Figure 3E). However, in the *Hmx2*$^{-/-}$;*Hmx3*$^{-/-}$ otic vesicle, *Dlx5* is exclusively expressed in the medial face that is destined to form the endolymphatic duct (Figure 3F). Ectopic expression of *Dlx5* in the dorsolateral aspect manifested by the *Hmx2*$^{-/-}$ mutant inner ear can no longer be seen in the *Hmx2*$^{-/-}$;*Hmx3*$^{-/-}$ mutants (Figure 3F and Wang et al., 2001). *Foxg1* (previously known as *Brain Factor 1*), a winged helix transcription factor, is restricted to the ganglionic cells and to the dorsomedial otic epithelium in the developing wild-type inner ear (Figure 3A; Hebert and McConnell, 2000). In the *Hmx2*$^{-/-}$;*Hmx3*$^{-/-}$ mutants, the lateral aspect of the dorsal otic vesicle also is positive for *Foxg1* (arrowhead in Figure 3B). Netrin1, a member of the laminin-related secreted proteins, is expressed in the nonsensory epithelium destined to form the fusion plate (Salminen et al., 2000). Remarkably, the *Netrin1*-positive domains in both the lateral and medial (Figure 3G) aspects of the wild-type otic vesicle were lost in the *Hmx2*$^{-/-}$;*Hmx3*$^{-/-}$ inner ears

(Figure 3H). Since no effect on *Netrin1* expression has been observed in either *Hmx2* or *Hmx3* single mutants, absence of this gene in the double mutants indicates that *Hmx2* and *Hmx3* function in a mutually redundant way in regulating *Netrin1* expression in the developing inner ear. Taken together, these data indicate that the molecular identity of the dorsolateral aspect of the mutant otic vesicle is dramatically altered following the loss of both *Hmx2* and *Hmx3*.

Defective Neuroendocrine System in *Hmx2*$^{-/-}$;*Hmx3*$^{-/-}$ Mutant Mice

In addition to their expression in the developing inner ear, both *Hmx2* and *Hmx3* are extensively and identically expressed in many regions in the central nervous system, including the neural tube, and hypothalamus, as well as discrete domains in the mesencephalon, metencephalon, and myelencephalon, during embryogenesis (Wang et al., 2000). The overall size and body weight of the *Hmx2*$^{-/-}$;*Hmx3*$^{-/-}$ newborns were indistinguishable from their normal littermates (*Hmx2*$^{+/+}$;*Hmx3*$^{+/+}$ or *Hmx2*$^{+/-}$;*Hmx3*$^{+/-}$). Results obtained from skeletal preparations of the spinal canal and histological analysis on sections of neural tissue, as well as RNA situ hybridization, failed to reveal any morphological, cytological, or molecular abnormalities in the spinal cord, hindbrain, or midbrain (data not shown). However, postnatal progressive dwarfism together with subsequent lethality in the *Hmx2*$^{-/-}$;*Hmx3*$^{-/-}$ newborns suggested a possible correlation with *Hmx2* and *Hmx3* expression in the hypothalamus. Expression of *Hmx2* (which is identical to expression of *Hmx3*) in the hypothalamus was visualized by β-galactosidase staining of an E18.5 *Hmx2*$^{+/lacZ}$ brain (Figure 4Aa). In the anterior hypothalamus, *Hmx2* and *Hmx3* were principally expressed in the preoptic nucleus. Lower but significant levels of *Hmx2* and *Hmx3* expression were detected in the entire posterior hypothalamus with higher expression in the arcuate nucleus (ARN) and the lateral hypothalamic area (Figure 4Ab). Serum levels of growth hormone (GH) were assayed in P0 newborns, which revealed greater than a 40% ($p < 0.05$) reduction in circulating GH levels in the *Hmx2*$^{-/-}$;*Hmx3*$^{-/-}$ newborns relative to wild-type, suggesting a possible perturbation of the *Hmx2*$^{-/-}$;*Hmx3*$^{-/-}$ neuroendocrine system. Interestingly, the circulating levels of other neuropeptide hormones, such as thyroid stimulating hormone (TSH) or prolactin (PRL), did not show any significant difference between the *Hmx2*$^{-/-}$;*Hmx3*$^{-/-}$ and wild-type neonates (Figure 4Ac). When examined at P9, the time point past which no *Hmx2*$^{-/-}$;*Hmx3*$^{-/-}$ pup survived, the overall size of the arcuate nucleus was dramatically reduced likely owing to overall body growth retardation. The total number of neuronal cell bodies in the ARN was not altered significantly (wild-type, $n = 583 \pm 8.7$; *Hmx2*$^{-/-}$;*Hmx3*$^{-/-}$, $n = 587 \pm 26.7$; $p = 0.85$), and these cells were condensed in a smaller area within the mutant ARN as compared to wild-type, indicating that *Hmx2* and *Hmx3* themselves are not directly involved in the early determination of ARN neuron precursors (Figures 4Ad and 4Ae).

When the wild-type and *Hmx2;Hmx3* null pituitaries were examined, the anterior lobe was found to be severely affected in *Hmx2;Hmx3* null postnatal animals. Although there is an overall decrease in the total size of the pituitary and other organs in the *Hmx2;Hmx3* nulls (likely owing to a general decrease in body size), the dramatic reduction in size of the anterior pituitary suggested a possible cell type-specific loss in this tissue (Figures 4Af and 4Ag). Interestingly, the intermediate and posterior lobes of the pituitary seemed to develop proportionally to the overall body size of the *Hmx2;Hmx3* null pups.

Disturbed Hypothalamic-Pituitary Axis of the *Hmx2*$^{-/-}$;*Hmx3*$^{-/-}$ Mice at the Molecular Level

Growth hormone releasing hormone (GHRH) is produced by parvocellular neurons in the arcuate nucleus and adjacent ventromedial nucleus in the posterior hypothalamus of wild-type mice (Figure 4Ba). In the *Hmx2*$^{-/-}$;*Hmx3*$^{-/-}$ hypothalamus, expression of GHRH was completely abolished in the arcuate nucleus, whereas its mRNA expression in the VMN showed no signs of being affected (Figure 4Bb). Galanin, another neuropeptide hormone coexpressed with GHRH in the parvocellular neurons of the ARN, plays critical physiological roles in regulating food intake, memory, and learning, as well as sexual activity (Chan et al., 1996; Hohmann et al., 1998). Besides the ARN, *Galanin* mRNA is also detectable in the periventricular nucleus (PVN; arrowhead in Figure 4Bc) and the lateral hypothalamic area of the hypothalamus, as well as many other regions in the brain such as the hippocampus (data not shown). In the *Hmx2*$^{-/-}$;*Hmx3*$^{-/-}$ brain, cell groups coexpressing *Galanin* and *Hmx2/3* are affected, including the ARN and LHA where *Galanin* expression is abolished (Figures 6Bc and 6Bd). The expression of *Galanin* in the PVN of hypothalamus and other brain regions is unperturbed, suggesting the direct correlation between the absence of *Galanin* in the ARN and LHA and the loss of *Hmx2/3* in these same regions (arrowhead in Figure 4Bd; data not shown).

Homeobox gene *Gsh1* expression is predominantly located in the neuronal cell bodies in the arcuate nucleus and lateral hypothalamic area that overlaps with the *Hmx2* and *Hmx3* expression domains (Figures 4Ab and 4Be). Loss of *Gsh1* function abolished GHRH production, leading to severe postnatal growth retardation in the *Gsh1* null mice (Li et al., 1996). Intriguingly, *Gsh1* expression in the hypothalamus was lost in the *Hmx2*$^{-/-}$;*Hmx3*$^{-/-}$ mutant brain (Figures 4Be and 4Bf), indicating that *Gsh1* is a key mediator in regulating GHRH secretion, and this in turn is directed via *Hmx2* and *Hmx3*. *Gsh1* expression in other areas aside from the hypothalamus, such as the neural tube and forebrain, was unaffected by the inactivation of *Hmx2* and *Hmx3* (Valerius et al., 1995; data not shown).

The reduction in GH production in the *Hmx2*$^{-/-}$;*Hmx3*$^{-/-}$ brain may also be the result of upregulated levels of somatostatin (SS) and neuropeptide Y (NPY), two key antagonists of GH secretion (Kamegai et al., 1996). In the *Hmx2*$^{-/-}$;*Hmx3*$^{-/-}$ hypothalamus, NPY expression in the LHA and ARN, as well as SS expression in the PeN and ARN, is correctly maintained, indicating that the inhibitory feedback pathway regulating GH production remains intact (Figures 4Bg–4Bj). The homeobox gene *Otp* has been shown to be required for the terminal

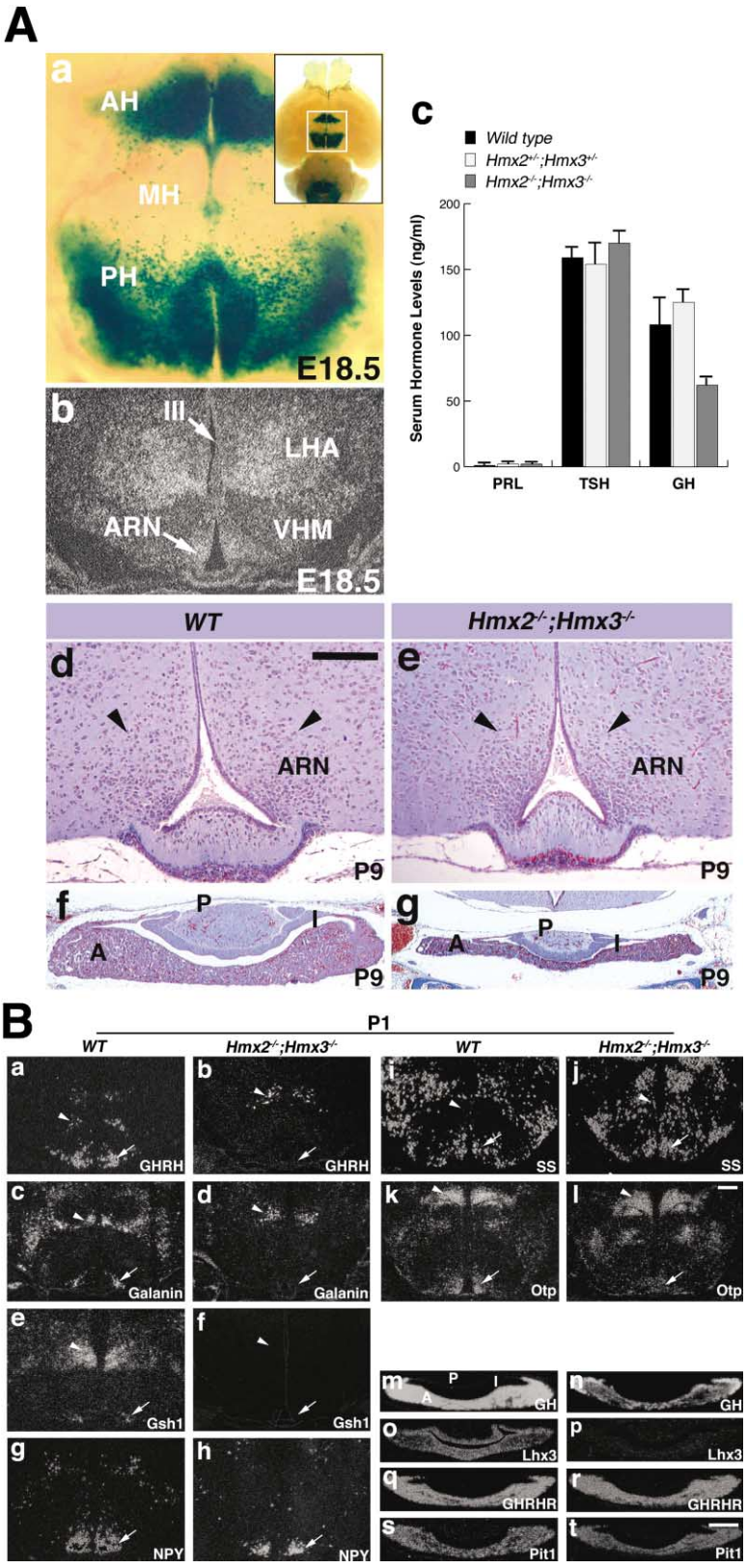

Figure 4. Defective Neuroendocrine System of the *Hmx2*$^{-/-}$;*Hmx3*$^{-/-}$ Mice

(A) Spatial expression pattern of *Hmx2* and *Hmx3* in the wild-type hypothalamus of E18.5 embryo (a and b). *Hmx2* and *Hmx3* show an identical pattern of expression in the CNS (Wang et al., 2000). Inset in (a) shows ventral view of a whole-mount *Hmx2*$^{lacZ+/-}$ brain examined by β-galactosidase activity. (a) is the high-power view of the boxed region shown in the inset. (b) In situ hybridization on a coronal section at the level of posterior hypothalamus showing the expression of *Hmx2*/*Hmx3* in the arcuate nucleus and the lateral hypothalamic area in the wild-type embryo at E18.5. (c) Circulating hormone levels of PRL, TSH, and GH were examined from wild-type, heterozygous, and *Hmx2*$^{-/-}$;*Hmx3*$^{-/-}$ neonates. Genotypes of specimens are indicated in the upper left corner of (c). (d to g) Abnormalities displayed by the *Hmx2*$^{-/-}$;*Hmx3*$^{-/-}$ hypothalamus and pituitary at postpartum day 9 (P9). Mallory's tetrachrome staining of coronal sections at comparable anatomic levels in the posterior hypothalamus of the wild-type and *Hmx2*$^{-/-}$;*Hmx3*$^{-/-}$ pups. Arrowheads in (d) and (e) mark the boundary of the arcuate nuclei. (f and g) Photographs shot at the same power showing the growth retardation of the entire *Hmx2*$^{-/-}$;*Hmx3*$^{-/-}$ pituitary and the degeneration of the anterior lobe. Physiological stages examined are indicated on the lower right corner of each panel. Genotype of each specimen shown in (d) to (g) is indicated on the top of each column. Scale bar in (d) refers to (d) to (g) and represents 100 μm.

(B) Perturbation of the hypothalamus-pituitary axis was examined at the molecular level by in situ hybridization. Genotype of *Hmx2; Hmx3* is listed on the top of each column and in situ probe employed is indicated at the lower right corner. Scale bars in (l) (refers to [a] to [l]) and t (refers to [m] to [t]) correspond to 50 μm.

Abbreviations: A, anterior lobe of pituitary; AH, anterior hypothalamus; ARN, arcuate hypothalamic nucleus; I, intermediate lobe of pituitary; LHA, lateral hypothalamic area; MH, medial hypothalamus; P, posterior lobe of pituitary; PH, posterior hypothalamus; III, third ventricle; VMH, ventromedial thalamic nucleus.

differentiation and maturation of many hypothalamic nuclei, including the anterior periventricular (aPV), paraventricular, and supraoptic nuclei (Acampora et al., 1999; Wang and Lufkin, 2000). In the *Hmx2*$^{-/-}$;*Hmx3*$^{-/-}$ newborns, *Otp* expression in the above areas is unaffected (Figures 4Bk and 4Bl).

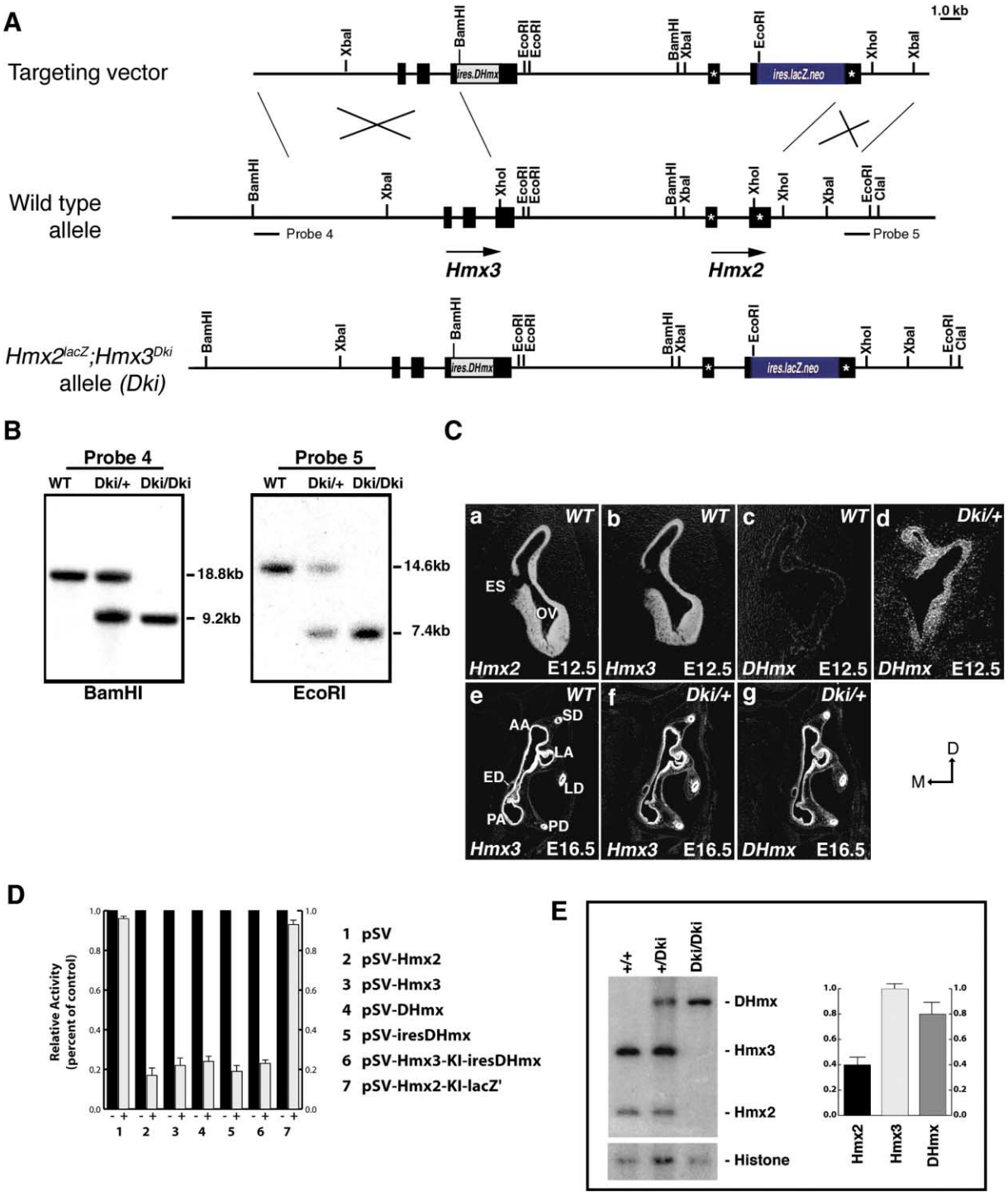

Figure 5. Targeting of *DHmx* to *Hmx3* and *lacZ* to *Hmx2*

(A) Gene targeting knockin strategy for generation of the $Hmx2^{lacZ/lacZ};Hmx3^{Dki/Dki}$ allele. Homologous recombination of the targeting vector (shown in the top line) leads to the insertion of *ires.DHmx* into the *Hmx3* gene and *ires.lacZ.neo* cassette into the *Hmx2* gene ($Hmx2^{lacZ/lacZ};Hmx3^{Dki/Dki}$ allele shown in the bottom line, abbreviated as *Dki*).

(B) Tail DNA from mice of the indicated genotypes subjected to Southern blot. Insertion of the *ires.DHmx* cassette introduced an additional BamHI site into the homeobox of *Hmx3* and integration of *ires.lacZ.neo* cassette into the *Hmx2* homeobox generated an extra EcoRI site.

(C) In situ hybridization on paraffin sections from E12.5 wild-type and $Hmx2^{+/lacZ};Hmx3^{+/Dki}$ embryos was employed to confirm that the *Drosophila Hmx* is correctly expressed in the same temporal and spatial pattern as the endogenous *Hmx2* and *Hmx3* genes. Genotypes of each sample are indicated at the top of each panel; antisense in situ probes are indicated at the bottom left of each panel.

(D) Transfection analysis of Hmx constructs transcriptional activity in primary mouse embryo cells. pSV vector alone (pSV, lane 1) or pSV vector containing the indicated ORFs or cDNAs of Hmx2 (lane 2), Hmx3 (lane 3), DHmx (lane 4), iresDHmx (lane 5), Hmx3 cDNA with a knockin

Owing to the absence of *GHRH* transcripts in the hypothalamus, *GH* gene expression in the anterior pituitary was significantly downregulated, but not completely turned off (Figures 4Bm and 4Bn). The vestiges of *GH* transcripts suggest that alternative regulatory pathway (i.e., local signals from the anterior pituitary) other than GHRH may still be effective to maintain the basal level of GH expression and secretion. The LIM-homeodomain-containing gene *Lhx3* plays a critical role in the differentiation and proliferation of almost all pituitary cell lineages except the corticotropes (Sheng et al., 1996). Inactivation of *Hmx2* and *Hmx3* results in the absence of *Lhx3* expression in the neonatal pituitary (Figures 4Bo and 4Bp). Even though *GHRH* expression is abolished in the hypothalamus and *GH* is dramatically downregulated in the anterior pituitary, GHRH receptors are still present in the anterior pituitary (Figures 4Bq and 4Br). No difference in *Pit1* expression was seen between the wild-type and $Hmx2^{-/-};Hmx3^{-/-}$ pituitaries, suggesting that the overall cellular composition of the anterior pituitary is not discernibly affected by the inactivation of the *Hmx2* and *Hmx3* genes (Figures 4Bs and 4Bt).

Substitution of Mouse *Hmx3* with *Drosophila Hmx* and Mouse *Hmx2* with *lacZ* In Vivo Results in Developmental Rescue of the $Hmx2^{-/-};Hmx3^{-/-}$ Mutant Neuroendocrine System and Inner Ears

We generated knockin mouse lines where the *Drosophila Hmx* (*DHmx*) coding sequence was placed under the transcriptional control of the *Hmx3* locus by inserting the *DHmx* cDNA fitted with an IRES (Li et al., 1997) into the coding region of the murine *Hmx3*. At the same time, the reporter and selection cassette *lacZ.neo* was inserted into the coding sequence of *Hmx2*, thus generating an *Hmx2;Hmx3* null allele that expresses *Drosophila Hmx* under the control of murine *Hmx3* and *lacZ* under the control of *Hmx2*. $Hmx2^{+/lacZ};Hmx3^{+/Dki}$ mice and wild-type mice were indistinguishable in all biological aspects examined. All $Hmx2^{lacZ/lacZ};Hmx3^{Dki/Dki}$ mice derived from two independent ES clones, regardless of their genetic backgrounds, showed classic vestibular defects as indicated by hyperactivity, head tilting, and circling activity with variable penetrance from 2 weeks after birth. $Hmx2^{lacZ/lacZ};Hmx3^{Dki/Dki}$ pups showed no difference in their body size and weight from their wild-type or $Hmx2^{+/lacZ};Hmx3^{+/Dki}$ littermates up to 6 weeks after birth.

Figure 5C shows that the *DHmx* mRNA faithfully recapitulated the expression of *Hmx3* in the vestibular portion of the otic vesicle in $Hmx2^{+/lacZ};Hmx3^{+/Dki}$ in early and late stage embryos when a specific probe derived from the 3′UTR of *DHmx* was used for in situ hybridization (Figures 5Ca to 5Cg). Meanwhile, when examined in whole-mount embryos, β-galactosidase activity was detected in all *Hmx2*-expressing domains in a correct temporal fashion, indicating that the *lacZ* reporter gene is strictly controlled by the regulatory elements of the endogenous *Hmx2* in the $Hmx2^{+/lacZ};Hmx3^{+/Dki}$ allele. Therefore, by comparing the phenotypes of the $Hmx2^{lacZ/lacZ};Hmx3^{Dki/Dki}$ mice to those of $Hmx2^{-/-};Hmx3^{-/-}$ mice, any phenotypic differences exhibited by the $Hmx2^{lacZ/lacZ};Hmx3^{Dki/Dki}$ mice can be attributed to the replacement of the mouse *Hmx3* gene with the *Drosophila Hmx* gene and can help us to determine to what extent the biochemical function of the DHmx/Hmx3 protein has been retained during evolution. The relative transcriptional activity of the Hmx2, Hmx3, and DHmx proteins and the efficacy of Hmx protein production from the engineered mutant alleles described here were assayed using an Hmx consensus binding site reporter construct (Amendt et al., 1999) in transfected mouse primary embryo cells (Figure 5D). Equal amounts of *Hmx2*, *Hmx3*, and *DHmx* expression plasmid show a nearly equivalent level of transcriptional repressive activity (Figure 5D, lanes 1–4). The addition of the IRES sequence to *DHmx* did not appreciably change the level of DHmx protein production, either relative to the native ATG or when inserted into the *Hmx3* coding sequence (Figure 5D, lane 4–6), suggesting that the IRES functions as efficiently as the native ATG and produces neither significantly higher nor lower levels of protein product relative the to wild-type open reading frame. As expected, the insertion of the *lacZ* (lacZ′ inverted) gene into the *Hmx2* coding region completely abolished Hmx2 transcriptional activity (Figure 5D, lane 7). The relative amounts of *Hmx2*, *Hmx3*, and *DHmx* transcripts were assayed in E12.5 wild-type, heterozygous, and homozygous $Hmx2^{lacZ/lacZ};Hmx3^{Dki/Dki}$ embryos (Figure 5E). *DHmx* and *Hmx3* mRNA transcripts accumulate to approximately the same levels in the corresponding wild-type, heterozygous, and null embryos, suggesting that *DHmx* does not have a significantly different mRNA half-life relative to *Hmx3*, nor (as expected) is it transcribed at an appreciably different rate from wild-type *Hmx3* in the $Hmx3^{Dki}$ locus.

No defects were discernable in the $Hmx2^{+/lacZ};Hmx3^{+/Dki}$ inner ear compared to wild-type, indicating that one wild-type copy of the *Hmx2;Hmx3* allele is sufficient to ensure the normal developmental program of the inner ear (Figure 6Aa). Consistent with the behavioral variations described above, the $Hmx2^{lacZ/lacZ};Hmx3^{Dki/Dki}$ inner ear phenotype showed a variable degree of penetrance or phenotypic rescue. Figures 6Ae and 6Af show the dissected $Hmx2^{lacZ/lacZ};Hmx3^{Dki/Dki}$ inner ears stained for

---

of iresDHmx identical to the Hmx3 portion of the Dki allele (lane 6), and Hmx2 cDNA with a knockin of lacZ (inverted) identical to the Hmx2 portion of the Dki allele (lane 7).

(E) Left, RNase protection analysis of *Hmx2*, *Hmx3*, and *DHmx* mRNA expression levels in individual E12.5 wild-type, $Hmx2^{+/lacZ};Hmx3^{+/Dki}$, and $Hmx2^{lacZ/lacZ};Hmx3^{Dki/Dki}$ whole embryos. *DHmx* mRNA levels are similar to either *Hmx2* or *Hmx3* mRNA levels. Histone mRNA is employed as a control for mRNA quality and quantity. Right, relative mRNA levels per allele of *Hmx2, Hmx3*, and *DHmx (Dki)* corrected for mRNA concentration, probe-specific activity, and allele dosage from three independent experiments. The median level of *Hmx3* expression is set at 1.0 and the values shown represent a combination of values from wild-type versus $Hmx2^{lacZ/lacZ};Hmx3^{Dki/Dki}$ levels as well as levels observed within $Hmx2^{+/lacZ};Hmx3^{+/Dki}$ embryos as the two groups of values are essentially identical. Statistical analysis was performed using an unpaired Student's t test. Error bars indicate standard deviations.

Abbreviations: A, anterior; AA, anterior ampulla; D, dorsal; Dki, $Hmx2^{lacZ};Hmx3^{Dki}$; ED, endolymphatic duct; ES, endolymphatic sac; OV, otic vesicle; L, lateral; LA, lateral ampulla; LD, lateral duct; M, medial; PA, posterior ampulla; PD, posterior duct; SD, superior duct.

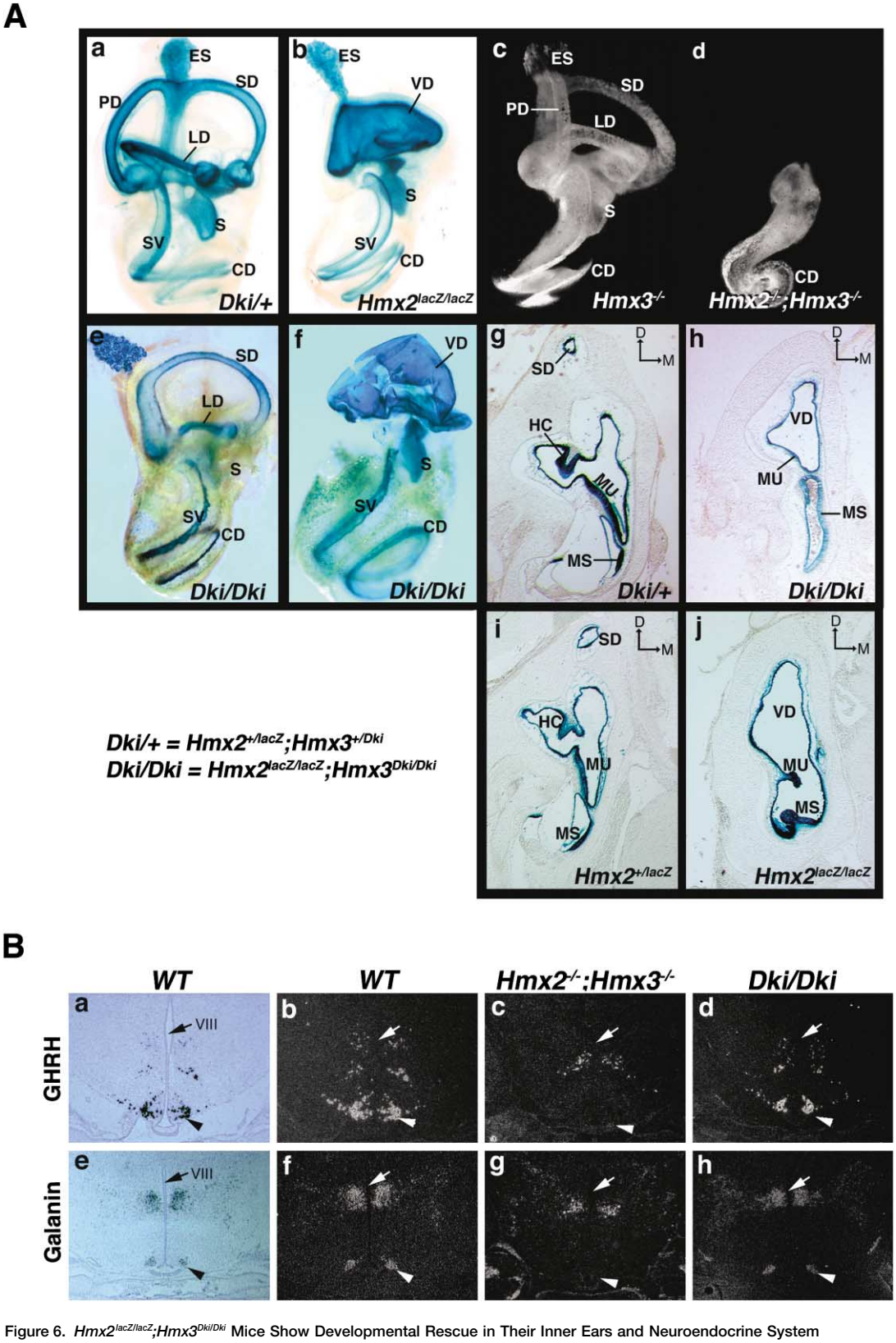

Figure 6. *Hmx2*$^{lacZ/lacZ}$;*Hmx3*$^{Dki/Dki}$ Mice Show Developmental Rescue in Their Inner Ears and Neuroendocrine System

(A) The inner ear phenotype in the mice rescued by *Drosophila Hmx* shows partial rescue and variable penetrance. (a) A β-galactosidase-stained *Hmx2*$^{+/lacZ}$;*Hmx3*$^{+/Dki}$ inner ear, of which the gross morphology is indistinguishable from a wild-type inner ear. (b) Structural alteration in the *Hmx2*$^{lacZ/lacZ}$ inner ear as shown by β-galactosidase activity. (c and d) *Hmx3*$^{-/-}$ and *Hmx2*$^{-/-}$;*Hmx3*$^{-/-}$ inner ear morphology visualized by paint filling, respectively. (e and f) Rescue of the inner ear phenotype when *DHmx* is placed under the control of the *Hmx3* locus. (g and h) Histological analysis of the rescued inner ear phenotype in the *Hmx2*$^{lacZ/lacZ}$;*Hmx3*$^{Dki/Dki}$ mice. Inner ears stained by β-galactosidase activity were

Table 1. Comparison of Various Parameters in *Hmx2*, *Hmx3*, *Hmx2;Hmx3*, and *Hmx2$^{lacZ/lacZ}$;Hmx3$^{Dki/Dki}$* Homozygous Mutant Inner Ears at E18.5

	Phenotype						
Genotype	Semicircular Canals	Cristae	Utricle/Saccule	Macular Sacculus	Macula Utriculus	Vestibular Ganglion	Spiral Ganglion
Hmx2$^{-/-}$	VD	loss by 68%	fused	normal	loss by 63%	loss by 51%	normal
Hmx3$^{-/-}$	normal	no horizontal crista	fused	loss by 13%	loss by 35%	reduced in number	normal
Hmx2$^{-/-}$/*Hmx3*$^{-/-}$	absent	absent	absent	absent	absent	absent	normal
Hmx2$^{lacZ/lacZ}$;Hmx3$^{DKi/DKi}$	VD, SD, and LD	absent	distinct chambers	normal	remnant discernable	reduced in number	normal

β-galactosidase. In embryos with the strongest penetrance, the superior semicircular duct appeared to be fully developed despite the absence of an associated ampulla (Figure 6Ae). The lateral semicircular duct was remarkably shortened and its associated ampulla was notably reduced in size. Interestingly, no distinguishable posterior semicircular duct was present in the *Hmx2$^{lacZ/lacZ}$;Hmx3$^{Dki/Dki}$* vestibular labyrinth. Instead, a large vesicle connecting the posterior ends of both the superior and lateral semicircular ducts was seen in the posterior labyrinth, suggesting that the otic epithelial cells destined for the posterior semicircular duct failed to undergo correct outgrowth and fusion during inner ear morphogenesis (Figure 6Ae). As for *Hmx2$^{lacZ/lacZ}$;Hmx3$^{Dki/Dki}$* inner ears showing the weakest penetrance, the gross morphology of the *Hmx2$^{lacZ/lacZ}$;Hmx3$^{Dki/Dki}$* vestibule was very similar to that of *Hmx2$^{lacZ/lacZ}$* in that the distinctive semicircular ducts were replaced by primordium diverticula (Figures 6Ab and 6Af). However, unlike the *Hmx2$^{lacZ/lacZ}$* vestibule, the endolymphatic duct failed to form in the *Hmx2$^{lacZ/lacZ}$;Hmx3$^{Dki/Dki}$* inner ears (Figure 6Af). Relative to the *Hmx2*$^{-/-}$*; Hmx3*$^{-/-}$ mutant inner ear, the gross structures of the *Hmx2$^{lacZ/lacZ}$;Hmx3$^{Dki/Dki}$* inner ear were significantly rescued by the expression of *Drosophila Hmx* from the *Hmx3* locus since the entire vestibule is normally destined to degenerate in the *Hmx2*$^{-/-}$*;Hmx3*$^{-/-}$ mutants (Figures 6Ad–6Af). The vestibular phenotype of the *Hmx2$^{lacZ/lacZ}$;Hmx3$^{Dki/Dki}$* embryos reached a developmental level similar to or exceeding those displayed by the *Hmx2* null mutants (Figures 6Ah and 6Aj) except for the absence of the endolymphatic duct, indicating that the *DHmx* could fully substitute for murine *Hmx3* during development of the vestibule. However, the developmental defects present in the *Hmx2$^{lacZ/lacZ}$;Hmx3$^{Dki/Dki}$* inner ear were still more severe than those exhibited by *Hmx3*$^{-/-}$ mutants (which still have two wild-type alleles of *Hmx2*; Figures 6Ab, 6Ac, 6Ae, and 6Af), indicating that under these conditions, two alleles of *DHmx* were unable to functionally replace at the same time two alleles of *Hmx3* and two alleles of *Hmx2* function (the allele loss existing on a *Hmx2$^{lacZ/lacZ}$;Hmx3$^{Dki/Dki}$* null background).

Sectioning of β-galactosidase-stained inner ears confirmed that the rescued inner ear phenotype was nearly equivalent to that of the *Hmx2*$^{-/-}$ (Figures 6Ag and 6Ah). A transverse section at the level of the anterior *Hmx2$^{lacZ/lacZ}$;Hmx3$^{Dki/Dki}$* inner ear shown in Figure 6Ah indicates that the utricle and saccule developed into distinct endolymphatic chambers. Furthermore, the macula of the saccule appeared normal. However, the macula utriculus (i.e., the sensory epithelium in the utricle) failed to develop fully even though a slightly thickened region representing the remnant of these sensory cells could be identified in the corresponding area (Figures 6Ag and 6Ah). When the inner ear shown in Figure 6Ae was sectioned, the same extent of a rescued phenotype was observed in the utricle and saccule of the weakest rescued inner ear shown in Figure 6Af (data not shown). In all cases examined, no structures could be identified that represented the cristae ampullaris (Figures 6Ag and 6Ah); therefore, structures derived from the nonsensory epithelium showed a greater degree of morphological rescue in the *Hmx2$^{lacZ/lacZ}$;Hmx3$^{Dki/Dki}$* inner ears than those from sensory epithelium. All of these observations suggest that the sensory and nonsensory epithelial cells in the vestibule show differential responsiveness to the expression of *Drosophila Hmx*, leading to the observed rescue of the *Hmx2*$^{-/-}$*;Hmx3*$^{-/-}$ inner ear phenotype (Table 1).

In addition to the complete degeneration of the vestibule, the *Hmx2*$^{-/-}$*;Hmx3*$^{-/-}$ mice also had a disrupted neuroendocrine system as indicated by the loss of expression of the neuropeptides *GHRH* and *Galanin* (Figures 4Ba to 4Bd; Figures 6Bc and 6Bg). The prolonged life span as well as the later onset of growth retardation in the *Hmx2$^{lacZ/lacZ}$;Hmx3$^{Dki/Dki}$* mice suggested improvement in their endocrine system relative to *Hmx2*$^{-/-}$*; Hmx3*$^{-/-}$ mice. In situ hybridization demonstrated that the expression of both *GHRH* and *Galanin* was fully restored in the arcuate nucleus in the *Hmx2$^{lacZ/lacZ}$;Hmx3$^{Dki/Dki}$* hypothalamus (Figures 6Bd and 6Bh). The penetrance of this rescue by *DHmx* in the CNS was 100% among all individuals, regardless of their genetic backgrounds. Semiquantitative RT-PCR showed that no significant difference in the expression levels of both genes could be detected between the wild-type and *Hmx2$^{lacZ/lacZ}$; Hmx3$^{Dki/Dki}$* hypothalamus (data not shown), supporting

sectioned. Transverse section at the level of anterior *Hmx2$^{lacZ/lacZ}$;Hmx3$^{Dki/Dki}$* inner ears (h) was compared with that from the *Hmx2$^{+/lacZ}$;Hmx3$^{+/Dki}$* mice (g). Genotype of each specimen is indicated on the lower right corner in each panel. Abbreviations: CD, cochlear duct; D, dorsal; M, medial; MS, macula saccule; MU, macula utricle; SV, stria vascularis; VD, vestibular diverticulum. The remaining abbreviations as in Figure 1. (B) Full restoration of *GHRH* and *Galanin* expression in the *Hmx2$^{lacZ/lacZ}$;Hmx3$^{Dki/Dki}$* mice as analyzed by in situ hybridization. Genotype of each specimen is shown on the top of each column, and the in situ probe used is indicated on the left. Arrows show the third ventricle (III) and arrowheads indicate the arcuate nucleus in the hypothalamus. (a) and (e) are the corresponding light field views of the sections in (b) and (f), respectively.

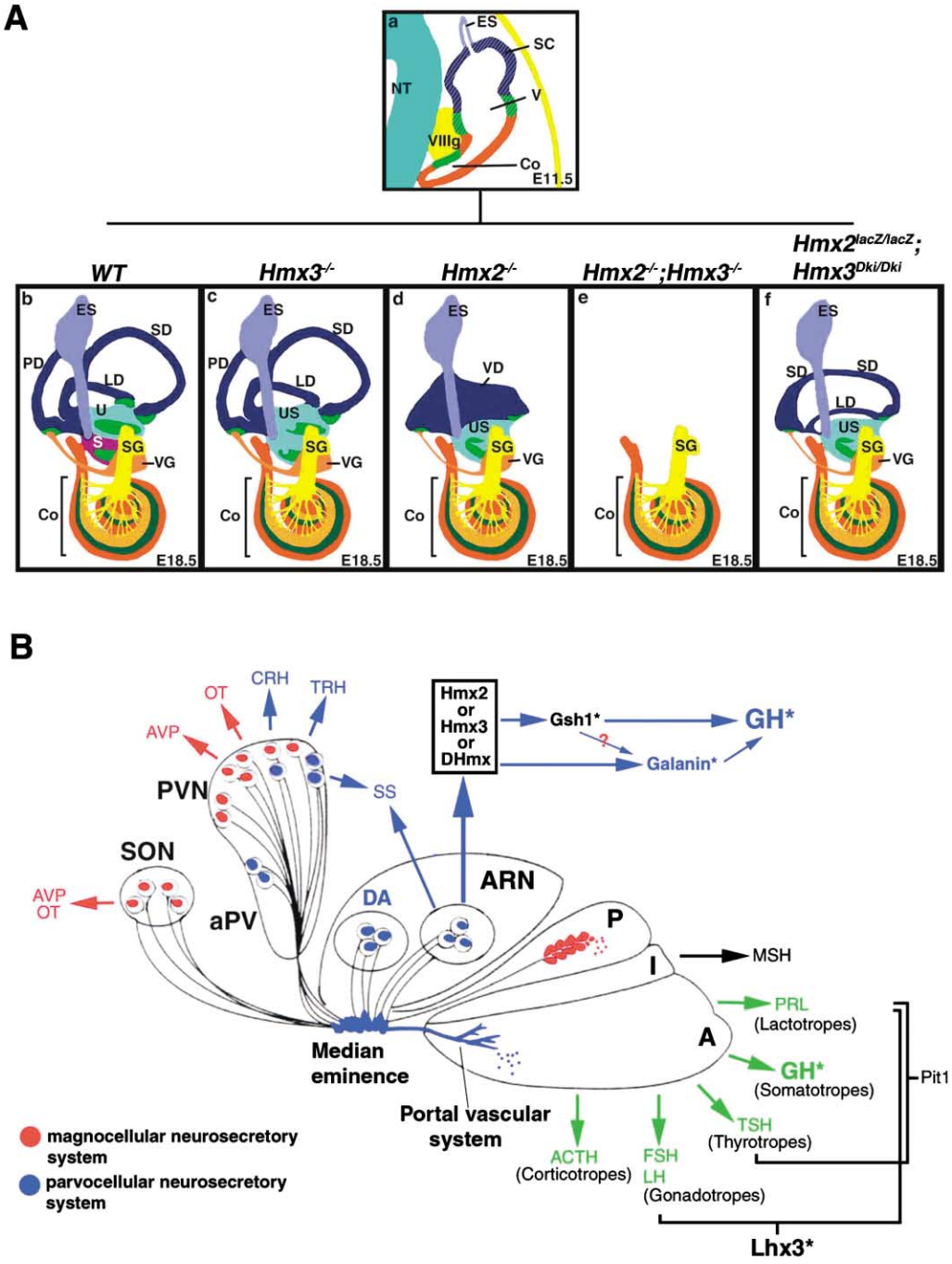

Figure 7. Schematic Summary of the Requirement of *Hmx2* and *Hmx3* in the Development of Inner Ear and Normal Function of Neuroendocrine System, as Well as the Functional Relationship between *Hmx2* and *Hmx3* Deduced from the Analysis of the *Hmx2;Hmx3* Null Mice

(A) (a) At E11.5, *Hmx2* and *Hmx3* are all expressed in the entire vestibular portion of the otic vesicle, including the prospective sensory patches and nonsensory epithelium that gives rise to the semicircular ducts and endolymphatic sac. (b) Medial-lateral view of a fully developed wild-type inner ear. The dark blue regions indicate the structures of the three semicircular ducts. The light blue domain shows the endolymphatic duct and the associated sac. The light green and purple regions mark the separated utricular and saccular spaces. The dark green domains indicate the sensory patches consisting of various hair cells in the vestibule and cochlea. Schematic representation of the vestibular (orange) and spiral (yellow) ganglia, as well as the corresponding nerves, is also indicated. The cochlear duct is shown in red. (c to e) Comparison of the defects displayed by the inner ear lacking the functional *Hmx3*, *Hmx2*, and *Hmx2/3* genes, respectively. (f) Dramatic rescue of the $Hmx2^{lacZ/lacZ};Hmx3^{Dki/Dki}$ inner ear. The backbone of the schematic diagram of (A) is modified from (Torres and Giraldez, 1998). Abbreviations: SG, spiral ganglion; US, utriculosaccular space; VIIIg, facial-acoustic ganglion; V, vestibule; VD, vestibular diverticulum. The remaining abbreviations as in Figures 1 and 3.

(B) Primary regions affected by the inactivation of *Hmx2* and *Hmx3* in the central nervous system are the arcuate nucleus in hypothalamus and the anterior lobe of pituitary. Functional *Hmx2* or *Hmx3* is required to regulate the release of peptide hormone such as GHRH and Galanin by the arcuate nucleus. The regulatory cascade by which *Hmx2* or *Hmx3* maintains the production of GHRH is accomplished via another

a complete phenotypic and molecular rescue by *DHmx* in this organ.

Discussion

The *Hmx* genes belong to a distinct homeobox gene family existing in a wide variety of species (Bober et al., 1994; Stadler et al., 1995; Stadler and Solursh, 1994; Wang et al., 1990). The expression profile of *Drosophila Hmx* in the developing brain suggests an ancestral function of this gene family in brain regionalization and neuronal cell fate specification (Wang et al., 2000). During evolution, the primordial *Hmx* gene was duplicated and the resulting *Hmx* genes were either clustered (*Hmx2* and *Hmx3*) or translocated (*Hmx1*) to different chromosomes as is seen in present-day mammals. *Hmx1*, *Hmx2*, and *Hmx3* function has been investigated by examining their developmental expression profile and analyzing the phenotypes of mice carrying null mutations in these genes. Nearly identical spatiotemporal expression patterns and amino acid identity of the DNA binding homeodomain, together with their close proximity on the chromosome, suggest that *Hmx2* and *Hmx3* may share some gene regulatory elements and also have overlapping physiological functions. Amino acid comparison and alignment of the Hmx2 (263 aa), Hmx3 (356 aa), and DHmx (273 aa) proteins show that all have strong conservation in the DNA binding homeodomain and overlapping λ-like repressor domain (reviewed in Lufkin, 2000). This is consistent with the functional analysis of all three proteins in cell transfection assays where they showed nearly equivalent transcriptional repression activity (Figure 5D) on a reporter construct containing consensus Hmx DNA binding motifs (Amendt et al., 1999). Both Hmx2 and Hmx3 also contain a POU-like domain (Klemm et al., 1994) and a proline-rich extension (Tompa, 2003) which are absent from DHmx and thus likely represent protein features that were acquired by the vertebrate genes following the split between vertebrates and arthropods, but prior to the tandem duplication of Hmx2 and Hmx3 on the chromosome. Interestingly, the positioning within the two proteins of the POU-like domains and proline-rich extensions vary between Hmx2 and Hmx3 (e.g., the proline-rich extension is located at the Hmx3 N terminus, whereas it is positioned in both the middle and C-terminal regions of Hmx2), suggesting that while being important for Hmx2 and Hmx3 function, the employment of these conserved domains may have diverged slightly during evolution and may contribute to the different functions of Hmx2 and Hmx3 in vivo. Hmx3 is unique in also containing a protein domain (orphan receptor domain, InterPro IPR003072) (Ohkura et al., 1996) which is not present in either Hmx2 or DHmx. This protein domain may represent a feature that was acquired by Hmx3 following the tandem duplication of *Hmx2* and *Hmx3* (or alternately was lost by Hmx2) and may contribute again to why these two proteins exert slightly different inner ear developmental functions despite being expressed in the same cell types during embryogenesis and why DHmx can rescue to a large extent most aspects of Hmx3 inner ear function, but not all.

The role of the *Hmx2* and *Hmx3* homeobox genes in inner ear development seems to be limited to the vestibular system (Figure 7A). Complete degeneration of the entire vestibular structures in the $Hmx2^{-/-};Hmx3^{-/-}$ inner ears clearly demonstrates that *Hmx2* and *Hmx3* do have overlapping functions with variable extent in every organ of the vestibule, including semicircular ducts, utricle and saccule, and the associated sensory receptor hair cells, as well as the endolymphatic duct. The ability of *DHmx* to rescue the $Hmx2^{-/-};Hmx3^{-/-}$ mutants in the $Hmx2^{lacZ/lacZ};Hmx3^{Dki/Dki}$ line appears to succeed better in otic cells which give rise to principally structural components of the inner ear rather than the smaller population of cells which comprise the sensory epithelium. Reduced cell-cycling or proliferation rates appear to be the underlying cellular mechanism responsible for faulty morphogenesis resulting from loss of *Hmx2* (Wang et al., 2001) which in turn becomes even more pronounced in the $Hmx2^{-/-};Hmx3^{-/-}$ mutants (except within the sensory epithelium, which shows a dramatic increase in apoptosis). Hence at the cellular level *DHmx* appears more effective at offsetting the effects of decreased cell proliferation rather than reversing any changes in elevated apoptotic rates.

The ancestral function of the *Hmx* gene family as suggested by the expression pattern of *Drosophila Hmx* and other species appears to be confined to the nervous system. Since no equivalent structures to the mammalian inner ear and neural retina are present in *Drosophila*, vertebrate *Hmx1*, *Hmx2*, and *Hmx3* expression in these sensory organs represents new roles acquired during evolution. Previous studies have demonstrated that the biological properties of genes separated by long periods of evolution can still be partially retained. For example, the *Drosophila engrailed* gene can rescue the brain defects of the *Engrailed1* (*En1*) mutant mice when substituted in place of mouse *En1*, but fails to rescue the limb defects or all the axial skeletal defects (Hanks et al., 1998). In a similar fashion, *Drosophila otd* was able to fully rescue *Otx1* in the developing mouse brain, but completely failed to improve any of the inner ear defects associated with *Otx1 loss-of-function* (Acampora et al., 1998). Taken together, these two previous examples support one theory that higher vertebrate structures such as the limb, skeleton, or inner ear arise during

homeobox gene, *Gsh1*. The secondary target organ for *Hmx2* and *Hmx3* is the anterior lobe of pituitary in which the transcription of Growth Hormone is downregulated significantly and *Lhx3* is shut down completely. (The basic structure of [B] is modified from Treier and Rosenfeld, 1996). Genes affected by the inactivated of *Hmx2* and *Hmx3* are marked with asterisks on their upper left. Abbreviations: A, anterior lobe of pituitary; ACTH, adrenocorticotropin; ARN, arcuate hypothalamic nucleus; aPV, anterior periventricular nucleus; AVP, arginine vasopressin; CRH, corticotropin-releasing hormone; DA, hypothalamic neuroendocrine dopaminergic neurons in the arcuate nucleus; FSH, follicle-stimulating hormone; GH, growth hormone; LH, luteinizing hormone; MSH, melanocyte-stimulating hormone; OT, oxytoxin; PRL, prolactin; PVN, paraventricular hypothalamic nucleus; SON, supraoptic nucleus; SS, somatostatin; TRH, thyrotropin-releasing hormone; TSH, thyroid-stimulating hormone. The rest of the abbreviations are as in Figure 4.

evolution principally from the acquisition of novel protein functions whereas evolutionary conserved organ systems like the brain continue to function largely via an evolutionarily conserved core of ancestral protein functions. In the case of the *Hmx* family, there seems to be a second alternative, as their contribution to the evolution of higher vertebrate organs appears to have resulted more from the acquisition of novel expression domains rather than primarily through novel protein functions.

DHmx was able to compensate fully for *Hmx3* in the murine CNS which in itself might have been anticipated, as the expression of *DHmx* is restricted exclusively to the fly CNS. *Hmx2* and *Hmx3* have a significant developmental overlap within the developing murine CNS, as either gene can compensate for the other during all aspects of patterning and cell-type specific differentiation of this organ, as the single gene *loss-of-function* mutations appear identical to wild-type. This compensation between *Hmx2* and *Hmx3* is not the case for the inner ear, where *Hmx2* and *Hmx3* have evolved minor specialized functions, as mutations in either gene give distinctly different morphological and cellular-based pathologies. The fact that *DHmx* is expressed at identical levels to *Hmx3* in the $Hmx2^{+/lacZ};Hmx3^{+/Dki}$ mice and can largely compensate for *Hmx3* in the developing vestibule indicates that whatever specialized functions have evolved for *DHmx* and the two murine genes since their divergence from a common ancestor, *DHmx* must have retained a core set of functions (such as protein cofactor interaction domains and control of downstream targets) also largely possessed by *Hmx3*.

Taken together, these results not only demonstrate that the molecular functions of the Hmx proteins have been significantly retained over several hundred million years of evolution, they also indicate that the emergence of highly complex organ systems like the mammalian inner ear can arise through the co-option of preexisting and conserved developmental genetic programs which are then employed in new embryonic tissues, rather than solely through the mutation and acquisition of additional protein functional domains or through the de novo construction of unprecedented genetic cascades.

Experimental Procedures

Construction of a Targeting Vector for Generating a Combined *Hmx2* and *Hmx3* Null Allele

The genomic organization of the *Hmx2* and *Hmx3* locus has been reported previously (Wang et al., 2001, 1998; Wang and Lufkin, 2000). A construct for disruption of both *Hmx2* and *Hmx3* was produced that deletes an 11 kb genomic fragment between the *Hmx2* and *Hmx3* homeoboxes. The 5′ targeting arm corresponds to an 11 kb BamHI+XhoI fragment containing the first and second exons, as well as part of the third exon of the *Hmx3* gene. The 3′ targeting arm is a 1.2 kb XhoI fragment containing part of the last exon of the *Hmx2* gene (Figure 1A). The above two genomic fragments were subcloned into the restriction sites in the polylinker of p662, a plasmid containing the GT1.2.neo cassette, thus generating plasmid pW71b. pW71b was linearized by NotI digestion, resulting in the targeting construct for the *Hmx2* and *Hmx3* double knockout as shown in Figure 1A.

Generation of Targeting Vector for Knockin of *Drosophila Hmx* into the Mouse *Hmx3* Locus and *lacZ* into the Mouse *Hmx2* Locus

The open reading frame and the 3′UTR of the *Drosophila Hmx* (Wang et al., 2000) were subcloned in frame with the translation start codon ATG in the internal ribosome entry site (IRES) (Li et al., 1997). The reporter gene *ires.lacZ.neo* was isolated from pW196a by XhoI (5′) and SalI (3′) digestions and inserted into the single XhoI site of pW212, generating plasmid pW215a. The 11 kb XhoI fragment deleted from pW211a was subsequently inserted back into pW215, finalizing the targeting vector (pW223a) for expressing *Drosophila Hmx* in place of the murine *Hmx3* and *lacZ* into the place of *Hmx2*.

ES Cell Manipulation and Production of Mutant Mice

ES cell (R1 and D3 [Gossler et al., 1986; Nagy et al., 1990]) transfections were performed essentially as previously described (Lufkin et al., 1991, 1993). ES clones containing a correctly targeted *Hmx2; Hmx3* locus were microinjected into C57BL/6J host blastocysts and chimeric mice were generated. Male chimeras were backcrossed to either C57BL/6J females for an outbred genetic background or to 129X1/SvJ (The Jackson Laboratory #000691) females for a coisogenic background.

Histology, RNA, Transfection, and Serum Analysis

Wild-type and $Hmx2^{-/-};Hmx3^{-/-}$ inner ears ($n > 3$ for each genotype) were injected with paint according to previously established methods (Martin and Swanson, 1993). Histology and measurements of areas were performed as described (Wang et al., 1998, 2001). Mallory's tetrachrome staining (Lufkin et al., 1992) and detection of β-galactosidase activity were performed as previously described (Frasch et al., 1995; Wang and Lufkin, 2000).

In situ hybridization on paraffin sections were performed as previously described (Wang et al., 1998). RNase protection analysis was performed on embryonic mRNA with PCR-generated fragments spanning the *lacZ* or *DHmx* insertion sites of *Hmx2* and *Hmx3*, respectively, or from the *DHmx* open reading frame (208 bp, 267 bp, and 359 bp protected RNAs, respectively) essentially as described (Wang et al., 1998). Transient transfection experiments were performed with 2.5 μg of TK-Hmx-Luciferase reporter construct (Amendt et al., 1999) and cotransfected with an equal amount of pSV-based Hmx expression construct (Green et al., 1988) and 0.5 μg of Actin-βgal (as internal control) into early passage primary mouse embryo cells and assayed as previously described (Amendt et al., 1999).

Measurement of the levels of serum GH, TSH, and PRL was kindly performed by A.F. Parlow, National Hormone and Peptide Program (NHPP), Harbor-UCLA Medical Center, CA. In brief, RIA for mouse PRL, TSH, and GH was performed using a double antibody method. For details, consult the NHPP site at www.humc.edu/hormones. Highly purified mouse PRL COV01-206, rat TSH COV01-205, and mouse GH AFP10783B were used as the iodinated ligands, rabbit anti-mouse PRL AFP131078, rat anti-mouse TSH AFP98991, and monkey anti-rat GH-RIA-5 (AFP) as the primary antibodies. Serum samples from at least three neonates of each genotype were measured.

Acknowledgments

We thank A.F. Parlow for performing the serum hormone assay, Peter Gruss, Kelly Mayo, Steven Potter, and Andreas Püschel for providing RNA in situ probes, and Brad Amendt for the TK-Hmx-Luc constructs. This work was supported in part by grants AR46471 and DE13741 from the NIH to T.L.

Received: December 23, 2003
Revised: June 16, 2004
Accepted: June 17, 2004
Published: August 9, 2004

References

Acampora, D., Avantaggiato, V., Tuorto, F., Barone, P., Reichert, H., Finkelstein, R., and Simeone, A. (1998). Murine Otx1 and *Drosophila* otd genes share conserved genetic functions required in invertebrate and vertebrate brain development. Development *125*, 1691–1702.

Acampora, D., Postiglione, M.P., Avantaggiato, V., Di Bonito, M., Vaccarino, F.M., Michaud, J., and Simeone, A. (1999). Progressive

impairment of developing neuroendocrine cell lineages in the hypothalamus of mice lacking the Orthopedia gene. Genes Dev. *13*, 2787–2800.

Amendt, B.A., Sutherland, L.B., and Russo, A.F. (1999). Transcriptional antagonism between Hmx1 and Nkx2.5 for a shared DNA-binding site. J. Biol. Chem. *274*, 11635–11642.

Bober, E., Baum, C., Braun, T., and Arnold, H.H. (1994). A novel NK-related mouse homeobox gene: expression in central and peripheral nervous structures during embryonic development. Dev. Biol. *162*, 288–303.

Chan, Y.Y., Grafstein-Dunn, E., Delemarre-van de Waal, H.A., Burton, K.A., Clifton, D.K., and Steiner, R.A. (1996). The role of galanin and its receptor in the feedback regulation of growth hormone secretion. Endocrinology *137*, 5303–5310.

Frasch, M., Chen, X., and Lufkin, T. (1995). Evolutionary-conserved enhancers direct region-specific expression of the murine Hoxa-1 and Hoxa-2 loci in both mice and *Drosophila*. Development *121*, 957–974.

Gossler, A., Doetschman, T., Korn, R., Serfling, E., and Kemler, R. (1986). Transgenesis by means of blastocyst-derived embryonic stem cell lines. Proc. Natl. Acad. Sci. USA *83*, 9065–9069.

Green, S., Issemann, I., and Sheer, E. (1988). A versatile in vivo and in vitro eukaryotic expression vector for protein engineering. Nucleic Acids Res. *16*, 369.

Greer, J.M., Puetz, J., Thomas, K.R., and Capecchi, M.R. (2000). Maintenance of functional equivalence during paralogous Hox gene evolution. Nature *403*, 661–665.

Hanks, M.C., Loomis, C.A., Harris, E., Tong, C.X., Anson-Cartwright, L., Auerbach, A., and Joyner, A. (1998). *Drosophila engrailed* can substitute for mouse *Engrailed1* function in mid-hindbrain, but not limb development. Development *125*, 4521–4530.

Hebert, J.M., and McConnell, S.K. (2000). Targeting of cre to the Foxg1 (BF-1) locus mediates loxP recombination in the telencephalon and other developing head structures. Dev. Biol. *222*, 296–306.

Hohmann, J.G., Clifton, D.K., and Steiner, R.A. (1998). Galanin: analysis of its coexpression in gonadotropin-releasing hormone and growth hormone-releasing hormone neurons. Ann. N Y Acad. Sci. *863*, 221–235.

Holland, P.W., and Garcia-Fernandez, J. (1996). Hox genes and chordate evolution. Dev. Biol. *173*, 382–395.

Kamegai, J., Minami, S., Sugihara, H., Hasegawa, O., Higuchi, H., and Wakabayashi, I. (1996). Growth hormone receptor gene is expressed in neuropeptide Y neurons in hypothalamic arcuate nucleus of rats. Endocrinology *137*, 2109–2112.

Klemm, J.D., Rould, M.A., Aurora, R., Herr, W., and Pabo, C.O. (1994). Crystal structure of the Oct-1 POU domain bound to an octamer site: DNA recognition with tethered DNA-binding modules. Cell *77*, 21–32.

Li, H., Zeitler, P.S., Valerius, M.T., Small, K., and Potter, S.S. (1996). Gsh-1, an orphan Hox gene, is required for normal pituitary development. EMBO J. *15*, 714–724.

Li, X., Wang, W., and Lufkin, T. (1997). Dicistronic LacZ and alkaline phosphatase reporter constructs permit simultaneous histological analysis of expression from multiple transgenes. Biotechniques *23*, 874–878.

Lufkin, T. (2000). Developmental control by Hox transcriptional regulators and their cofactors. In Transcription Factors, J. Locker, ed. (Oxford: Bios Scientific Publishers), pp. 215–235.

Lufkin, T., Dierich, A., LeMeur, M., Mark, M., and Chambon, P. (1991). Disruption of the Hox-1.6 homeobox gene results in defects in a region corresponding to its rostral domain of expression. Cell *66*, 1105–1119.

Lufkin, T., Mark, M., Hart, C.P., Dolle, P., LeMeur, M., and Chambon, P. (1992). Homeotic transformation of the occipital bones of the skull by ectopic expression of a homeobox gene. Nature *359*, 835–841.

Lufkin, T., Lohnes, D., Mark, M., Dierich, A., Gorry, P., Gaub, M.P., LeMeur, M., and Chambon, P. (1993). High postnatal lethality and testis degeneration in retinoic acid receptor alpha mutant mice. Proc. Natl. Acad. Sci. USA *90*, 7225–7229.

Martin, P., and Swanson, G.J. (1993). Desciptive and experimental analysis of the epithelial remodellings that control semicircular canal formation in the developing mouse inner ear. Dev. Biol. *159*, 549–558.

Meyer, A., and Schartl, M. (1999). Gene and genome duplications in vertebrates: the one-to-four (-to-eight in fish) rule and the evolution of novel gene functions. Curr. Opin. Cell Biol. *11*, 699–704.

Nagy, A., Gocza, E., Diaz, E.M., Prideaux, V.R., Ivanyi, E., Markkula, M., and Rossant, J. (1990). Embryonic stem cells alone are able to support fetal development in the mouse. Development *110*, 815–821.

Ohkura, N., Ito, M., Tsukada, T., Sasaki, K., Yamaguchi, K., and Miki, K. (1996). Structure, mapping and expression of a human NOR-1 gene, the third member of the Nur77/NGFI-B family. Biochim. Biophys. Acta *1308*, 205–214.

Rinkwitz-Brandt, S., Justus, M., Oldenettel, I., Arnold, H.H., and Bober, E. (1995). Distinct temporal expression of mouse Nkx-5.1 and Nkx-5.2 homeobox genes during brain and ear development. Mech. Dev. *52*, 371–381.

Salminen, M., Meyer, B.I., Bober, E., and Gruss, P. (2000). Netrin 1 is required for semicircular canal formation in the mouse inner ear. Development *127*, 13–22.

Sheng, H.Z., Zhadanov, A.B., Mosinger, B., Jr., Fujii, T., Bertuzzi, S., Grinberg, A., Lee, E.J., Huang, S.P., Mahon, K.A., and Westphal, H. (1996). Specification of pituitary cell lineages by the LIM homeobox gene *Lhx3*. Science *272*, 1004–1007.

Stadler, H.S., Padanilam, B.J., Buetow, K., Murray, J.C., and Solursh, M. (1992). Identification and genetic mapping of a homeobox gene to the 4p16.1 region of human chromosome 4. Proc. Natl. Acad. Sci. USA *89*, 11579–11583.

Stadler, H.S., and Solursh, M. (1994). Characterization of the homeobox-containing gene GH6 identifies novel regions of homeobox gene expression in the developing chick embryo. Dev. Biol. *161*, 251–262.

Stadler, H.S., Murray, J.C., Leysens, N.J., Goodfellow, P.J., and Solursh, M. (1995). Phylogenetic conservation and physical mapping of members of the H6 homeobox gene family. Mamm. Genome *6*, 383–388.

Tompa, P. (2003). Intrinsically unstructured proteins evolve by repeat expansion. Bioessays *25*, 847–855.

Torres, M., and Giraldez, F. (1998). The development of the vertebrate inner ear. Mech. Dev. *71*, 5–21.

Treier, M., and Rosenfeld, M.G. (1996). The hypothalamic-pituitary axis: co-development of two organs. Curr. Opin. Cell Biol. *8*, 833–843.

Valerius, M.T., Li, H., Stock, J.L., Weinstein, M., Kaur, S., Singh, G., and Potter, S.S. (1995). Gsh-1: a novel murine homeobox gene expressed in the central nervous system. Dev. Dyn. *203*, 337–351.

Wang, G.V., Dolecki, G.J., Carlos, R., and Humphreys, T. (1990). Characterization and expression of two sea urchin homeobox gene sequences. Dev. Genet. *11*, 77–87.

Wang, W., and Lufkin, T. (2000). The murine Otp homeobox gene plays an essential role in the specification of neuronal cell lineages in the developing hypothalamus. Dev. Biol. *227*, 432–449.

Wang, W., Van De Water, T., and Lufkin, T. (1998). Inner ear and maternal reproductive defects in mice lacking the Hmx3 homeobox gene. Development *125*, 621–634.

Wang, W., Lo, P., Frasch, M., and Lufkin, T. (2000). Hmx: an evolutionary conserved homeobox gene family expressed in the developing nervous system in mice and *Drosophila*. Mech. Dev. *99*, 123–137.

Wang, W., Chan, E.K., Baron, S., Van de Water, T., and Lufkin, T. (2001). Hmx2 homeobox gene control of murine vestibular morphogenesis. Development *128*, 5017–5029.

Yoshiura, K., Leysens, N.J., Reiter, R.S., and Murray, J.C. (1998). Cloning, characterization, and mapping of the mouse homeobox gene Hmx1. Genomics *50*, 61–68.